

The Non-Predictability of Mispredicted Branches using Timing Information

Ioannis Constantinou¹, Arthur Perais², and Yiannakis Sazeides¹

¹University of Cyprus

²Univ. Grenoble Alpes, CNRS, Grenoble INP, TIMA, Grenoble, France

Abstract

Branch misprediction latency is one of the most important contributors to performance degradation and wasted energy consumption in a modern core. State-of-the-art predictors generally perform very well but occasionally suffer from high Misprediction Per Kilo Instruction due to hard-to-predict branches.

In this work, we investigate if predicting branches using microarchitectural information, in addition to traditional branch history, can improve prediction accuracy. Our approach considers branch timing information (resolution cycle) both for older branches in the Reorder Buffer (ROB) and recently committed, and for younger branches relative to the branch we re-predict. We propose Speculative Branch Resolution (SBR) in which, N cycles after a branch allocates in the ROB, various timing information is collected and used to re-predict.

Using the gem5 simulator we implement and perform a limit-study of SBR using a TAGE-Like predictor. Our experiments show that the post-alloc timing information we used was not able to yield performance gains over an unbounded TAGE-SC. However, we find two hard to predict branches where timing information did provide an advantage and thoroughly analysed one of them to understand why. This finding suggests that predictors may benefit from specific microarchitectural information to increase accuracy on specific hard to predict branches and that overriding predictions in the backend may yet yield performance benefits, but that further research is needed to determine such information vectors.

1. Introduction

Despite its introduction 40 years ago by Smith [28], dynamic branch prediction remains not completely solved and a critical performance feature. A clear indication of the significance of branch predictors is the large real estate they occupy in modern cores, which is reported to be tens of KBs [8]. A branch prediction unit typically consists of a variety of predictors aimed at different types of branches, one of which predicts the direction of conditional branches (henceforth referred to as the branch predictor).

Although state-of-the-art accuracy is high, Chauhan et al. report that the performance of a Skylake-Like core would increase by 40% with a perfect branch predictor [4], highlighting the significant potential for improvement. This is supported by Figure 1 that depicts the (conditional) *Branch Mispredictions Per Kilo Instructions* (BMPKI) reduction and

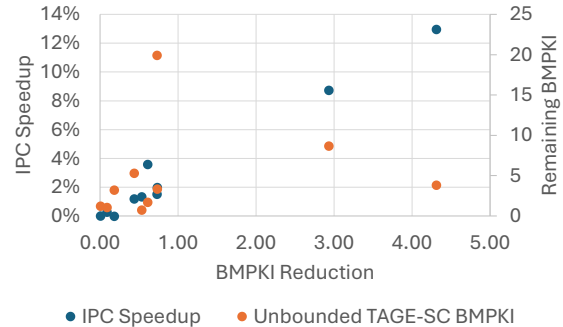


Figure 1: IPC Speedup and BMPKI Reduction of Unbounded TAGE-SC over a 64KB TAGE-SC (Secondary y-axis showing remaining BMPKI of Unbounded TAGE-SC for a specific BMPKI reduction compared to the baseline)

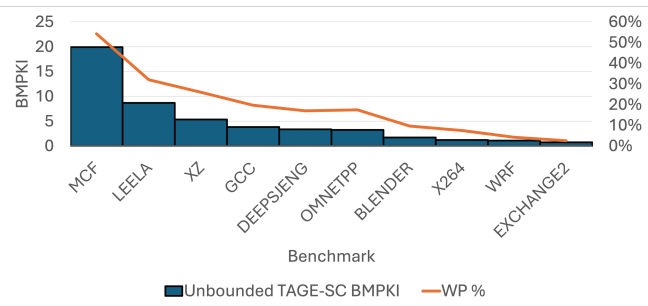


Figure 2: BMPKI of Unbounded TAGE-SC (primary y-axis) and % of Wrong Path Instructions (secondary y-axis)

Instruction Per Cycle (IPC) speedup of an unbounded TAGE-SC [22] over a 64KB TAGE-SC on a set of SPEC2K17 rate benchmarks simulated on gem5 [15] (experimental methodology is presented in Section 5). Clearly, there is a strong correlation between BMPKI reduction and performance. A potential solution to improve branch prediction accuracy is enhancing predictors table efficiency to reduce *aliasing*, e.g., through larger tables. However, even with effectively unbounded resources, many mispredicted branches remain (shown on the secondary y-axis in Figure 1), indicating the persistent challenge of Hard-To-Predict (H2P) branches.

High BMPKI is detrimental as it leads to a large fraction of wrong path instructions in the Reorder Buffer (ROB). Figure 2 highlights this relationship, showing that bench-

marks with high BMPKI also exhibit a high percentage of wrong path instructions, with over 50% in *mcf*. Such wrong path instructions represent wasted computation and energy, though they may offer some prefetching benefits [18]. This highlights the significant opportunity to improve performance, particularly for workloads with complex control flow that defeats advanced branch predictors.

Prior work has proposed diverse approaches for dealing with H2P branches, including hardware-software co-designs for data-dependent branches [1, 7, 27, 32] and hardware-only solutions like early misprediction detection using microarchitectural events that are more likely to occur in the wrong path (e.g., illegal opcode, nested mispredictions, etc.) [2]. A recent study employed offline-trained convolutional neural neural networks to dynamically detect key features in the branch history to use for prediction [31].

In this work, we first note that virtually all state-of-the-art predictors rely on *architectural* information to predict branches. A typical example is the global branch history, which represents the directions of past conditional branches and does not depend on the microarchitecture, but only on the program being executed. As a result, we explore the potential for exploiting correlation in *microarchitectural* information to predict branches. While there are many microarchitectural features that can be explored (e.g., cache misses, ROB occupancy, etc.), we focus on *timing*, i.e., the fact that at the moment we predict, some events have taken a given amount of *time*. The rationale behind this, is that timing can encode many specific events of the microarchitecture without having to explicitly watch each individual event. Another interesting aspect of this approach is that because the microarchitecture has a speculative window of "future" instructions, it is even possible to use the post-fetch timing behavior of younger instructions to (re-)predict older but not yet resolved branches, naturally leading to an overriding prediction approach. Using "future" – yet specific – information was suggested as a way to improve early resolution coverage by Armstrong et al. [2].

In summary, this paper first contributes a real-world example presenting why microarchitectural information and in particular timing can serve as an information vector for prediction. Second it proposes a microarchitectural flow for overriding the fetch predictor using microarchitectural information, *Speculative Branch Resolution*, or SBR. Third, it studies different combinations of microarchitectural information vectors to estimate the potential for SBR to provide meaningful MPKI gains. Although the results are generally negative – the microarchitectural information vectors used in our studies are not able to beat an impractically large TAGE-SC predictor – we provide a detailed analysis as to why and suggest cases where timing information may still have value.

2. Related Work

2.1. Mechanisms that Leverage Architectural Information

Most predictors rely on tying a program context to a given direction prediction. For instance, many predictors rely on the global branch history (n -bit vector with the direction of the n most recent conditional branches). These contexts are *architectural* in the sense that they depend only on the program semantics, and not on the hardware the program is being ran on. Many algorithms leveraging this type of information were proposed [5, 16, 24, 30], but this section only focuses on state-of-the-art predictors.

TAGE. This predictor [25] combines the global branch history and the path history (lower bits of past branch PCs) to index various tagged tables containing prediction counters. Each table is accessed with a different global history length, and the lengths follow a geometric series. This allows to capture correlation between distant branches, which are typically rare, while dedicating most of the storage to correlation between close branches. Improvements over a fine-tuned TAGE are generally achieved by combining it with "add on" predictors. One example is L-TAGE [20] where a loop predictor tries to identify regular loops with long loop counts. Another variant is TAGE-SC-L [22] that, in addition to the loop predictor, features a Statistical Corrector component which tries to find branches that are statistically biased and that TAGE does not always predict correctly. Another "add on" is the Inner Most Loop Iteration counter, or IMLI [26]. The IMLI counter is added in the statistical corrector and helps predicting branches that are encapsulated in the innermost loop body of multidimensional loops, by correlating the loop count with the encapsulated branch outcome.

Perceptron. The original perceptron-based predictor [13], and its refinements [10, 11, 29], use a different method of predicting branches based on neural networks. A single layer of perceptrons computes a prediction using a linear function that takes architectural information and per-PC weights as input to produce a prediction.

BranchNet. This predictor [31] uses a Convolutional Neural Network (CNN) architecture to predict branch directions. BranchNet is trained offline using program traces. At runtime, BranchNet predicts delinquent H2P branches, while the remaining branches are predicted by TAGE-SC-L. This hybrid approach can reduce the BMPKI of SPEC2017 benchmarks by 7.6% (and up to 15.7%) when compared to a standalone unlimited MTAGE-SC [23], and performs well because the CNN scheme can detect correlations in noisy and very long global histories without the need for exponentially large storage as the history grows.

Overriding Predictors. Ideally, branch predictors should provide the predicted direction of a branch in the cycle the branch is fetched, so that subsequent instructions can be fetched in the next cycle. Unfortunately, to achieve high accuracy, predictors use large tables and cannot meet such

timing requirement. As a result, branch prediction units can combine a small but fast reasonably accurate predictor with a large but slow and very accurate *overriding* predictor [12, 14, 24]. Although the latter is slower and incurs an override penalty, that penalty is much lower than the full branch misprediction penalty. Our approach can be seen as having an overriding predictor in the backend.

2.2. Mechanisms that Leverage Microarchitectural Information

Prophet/Critic Hybrid Branch Prediction. The prophet/critic hybrid branch predictor [6] has two predictors. The prophet is a classical predictor that correlates on the global branch history. The critic, on the other hand, re-predicts branches later in the pipeline, using information of "future" branches, that is, from predictions made by the prophet that correspond to branches that are younger than the one the critic is re-predicting. As a result, prophet/critic makes use of microarchitectural information because if critic overrides the prophet, then the predictions of the "future" branches used by the critic i) May not correspond to future correct control flow and ii) will disappear from the pipeline, despite having been used to generate a prediction.

Wrong Path Events. Armstrong et al. observe that rare events such as memory related exceptions (permission faults, unaligned accesses not supported in an ISA, etc.) can indicate that the pipeline is on the wrong path [2]. As a result, branch mispredictions can be resolved early if the proposed heuristic deems that a "problematic" event taking place does indeed indicate the control flow is incorrect. Unfortunately, "Wrong Path Events" (WPE) are rare and thus not many branches can be resolved early in this fashion. Our work proposes to find more frequent WPE to correlate on, namely the state of younger branches.

3. Motivation for Timing Information Vector

As previously mentioned, even with unbounded tables, state-of-the-art branch predictors are unable to predict correctly many branches and, as a result, alternative prediction techniques should be devised.

In this work, we adopt the suggestion by Armstrong et al. and enrich the type of information used to learn the behaviour of H2P branches [2]. More specifically, instead of using architectural information only (e.g., direction of past branches, address of past branches, etc.) as most of the existing predictors do, we also consider microarchitectural information such as branch timing information.

3.1. A Culprit

To illustrate why timing information can be used for prediction, and guide our selection of what timing information to use we analyze a H2P branch in the *mcf* workload of SPEC2017 CPU, which is a notoriously hard workload for control flow speculation and was one of the worst performers in Figure 2 (exact BMPKI numbers are provided in Table 2 in Section 5).

Listing 1 is an extract of the source code of the *spec_qsort* function, which contains six H2P branches with mispredict rates ranging from 11.1% to 31.3%. The *quick_sort* algorithm, given an unsorted table t of length n , determines a *pivot* value in the table that is used to move the values that are lower or equal to (resp. greater than) the pivot in the lower (resp. higher) part of the table. This process is recursively repeated on the derived table partitions. The Listing corresponds to the part of the algorithm that decides, according to the size of a partition, how to select the pivot: For short partitions, $n < 7$ (lines 4-9), it uses insertion sort to sort a partition and end the recursion.

For $n \geq 7$, it partitions the table and recurses using sampling for pivot selection as follows:

- For $n = 7$ (Line 10), use the value in $t[n/2]$ (value in the middle of the unsorted partition),
- For $n \leq 40$ (Line 12-21), use the median of $t[0], t[n/2], t[n - 1]$,
- For $n > 40$ (Line 15-20), use a more complex selection from 9 values

Branch A (Line 14), which checks if $n > 40$, is the H2P branch we focus on and its mispredict rate is 18.6%. Note that *spec_qsort* includes a recursive call to itself with its lower partition as parameter and a goto statement to iterate over part of the *spec_qsort* function when it returns from the recursive call to process the upper partition (thus avoiding the overhead of some recursive calls). As result, each function invocation may execute branch A multiple times with a recursive call between different executions of branch A.

```

1 void spec_qsort(void *a, size_t n, size_t es, cmp_t *cmp){
2 ... // Skipping some lines of code ...
3 loop:
4     if (n < 7) {
5         for(pm = (char *)a + es; pm < (char *)a + n * es;
6             pm += es)
7             for (pl = pm; pl > (char *)a & cmp(pl - es, pl)
8                 > 0; pl -= es)
9                 swap(pl, pl - es);
10    return;
11 }
12 pm = (char *)a + (n / 2) * es;
13 if (n > 7) {
14     pl = (char *)a;
15     pn = (char *)a + (n - 1) * es;
16     if (n > 40) { // Branch A
17         d = (n / 8) * es;
18         pl = med3(pl, pl + d, pl + 2 * d, cmp);
19         pm = med3(pm - d, pm, pm + d, cmp);
20         pn = med3(pn - 2 * d, pn - d, pn, cmp);
21     }
22     pm = med3(pl, pm, pn, cmp);
23 }
24 ... // Skipping some lines of code that
25 ... // perform the partitioning and update
26 ... // local variables pa, pb, pc, pd, pn...
27 if ((r = pb - pa) > es)
28     spec_qsort(a, r / es, es, cmp);
29 if ((r = pd - pc) > es) { // Branch B
30     /* Iterate rather than recurse to save stack space */
31     a = pn - r;
32     n = r / es;
33     goto loop;
34 }
```

Listing 1: Source code of *spec_qsort* in *mcf*

3.2. Analysis

Figure 3 reports some statistical properties of committed instances of branch A, as a function of the number of cycles

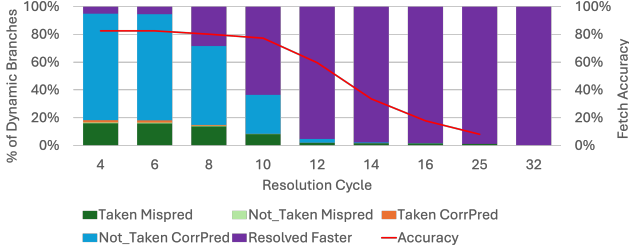


Figure 3: Taken and Not-Taken Correct Predictions and Mispredictions of Branch A as a function of resolution time (normalized to the total executions of this branch)

that elapsed since the branch was allocated in the ROB (x-axis) normalized to the total number of committed instances of branch A. By cycle four: 5.2% of instances have resolved, 76.8% are unresolved and will eventually be not-taken and predicted correctly, 1.7% are unresolved and will be taken and predicted correctly, 0.5% are unresolved and will be not-taken and mispredicted and finally, 16.0% are unresolved and will be not-taken and mispredicted. What we observe is that the *if* statement is mostly false (corresponding to not-taken branch A) and when it is true (A taken), it is almost always mispredicted. As the number of elapsed cycles after allocation in the ROB – *post-alloc* – increases the number of branches that remain unresolved decreases from 95.4% in cycle 4 to 71.6% in cycle 8, 2.3% in cycle 14, 1.7% in cycle 16 and 1.2% in cycle 25 (a handful remain unresolved past cycle 32). The key observation here is that the longer an instance of A remains unresolved, the more likely it is to be mispredicted! The Figure shows that the accuracy (secondary y-axis) decreases from 82.6% in cycle 4, to 80.1% in cycle 8, to 33.6% in cycle 14 and 17.8% and 7.8% in cycles 16 and 25, i.e., the large majority of instances that remain unresolved for 14 or more cycles are mispredicted.

Further investigation first revealed that the corresponding *if* statement line 14 is mostly false (i.e., n is generally less than or equal to 40) because, assuming the *spec_qsorth* partitions are perfectly balanced, then checking for a given size of partition p , as branch A tests, will converge to be true $\frac{1}{p}$ times.¹ For instance for $n = 41$ and table size greater than 1000 we expect around 2.5% of the instances of branch A to be true. The reason that the branch is true around 18% is because the *spec_qsorth* stops partitioning when the partition size is < 7 and uses insertion sort instead. Next, we focused on why this *if* is mostly false and branch A is mispredicted when it takes more than 14 cycles to resolve.

We observe that on occasions, when branch A is executed following a return from a recursive call, its execution is slower (Figure 3) for values of n greater than 40. This is due to the eviction of the local variables that the branch

1. Assuming a perfect binary tree with each node, except the root, representing a quick_sort partition of a table with size 2^n , then there are $2^{n+1}-2$ partitions in total, each with half the size of its parent node. In such tree, the fraction of nodes with partition size greater than or equal to 2^k is given by $1 - 2^n/2^k * (2^{k+1} - 2)/(2^{n+1} - 2)$ which simplifies to $1/2^k$ assuming 2^{n+1} is much larger than 2.

tests from the L1D. This is more likely to occur for larger values of n due to the amount of data being accessed: each arc records in the table to be sorted is 72 bytes, and the deeper recursion increases the number of allocated stack frames. Furthermore, when we are in a *spec_qsorth* invocation with value of n greater than 40 we expect for branch A to be executed *at least* seven times (this number depends on how well balanced the partitions are as we recurse through the data) until we return back to this function invocation, and all of these seven tests outcomes to be false, because at least seven resulting partitions will have length less than 40. This means that the predictor is trained multiple times with the information that branch A's outcome ($n > 40$) is false and as a result, when we return to the invocation with value of n equal to 40, the branch is usually mispredicted.

The discussion so far established that the number of cycles branch A remains unresolved can help detect whether it is mispredicted and, therefore, that timing information of microarchitectural events can serve as a source of information for branch prediction. However, at least for this example, the potential of this approach is rather limited since only a fraction of the mispredicted instances of A remain unresolved after cycle 12 (see Figure 3), and for earlier cycles, most instances are predicted correctly. However, one can also correlate on the timing behavior of other branches. Specifically, in this example, between the time we return from a recursive call and the execution of A, six branches are often executed, with each of these branches testing information contained in local variables. As a result, correlating on the timing behavior of some or all of these branches can actually serve us better because a possible mispredict by any of these branches may hide the cache delay of the inputs of branch A. In fact, we found that whenever the *if* statement corresponding to branch B line 27 is true (execute the goto), and its resolution required more than 20 cycles (roughly the latency of the L2 cache), branch A is mispredicted 82% of the time. Conversely, when the *if* statement is true but B resolution is less than 20 cycles, branch A is only mispredicted 15% of the time.

3.3. Implications and Key Parameters

The previous example established that the timing of a branch – as far as how many cycles it remains unresolved post allocation in the ROB – can serve as an information vector for prediction for itself and for other branches. This vector can then be used to resolve branches after a number of cycles to reduce their misprediction penalty.

A key parameter of a timing based prediction approach is the number of cycles to wait to re-predict a branch. Beyond its accuracy and coverage implications, the re-predict cycle is important for the performance gain or penalty of such a scheme. We illustrate this with an example: when branch A remains unresolved for 16 cycles after it is allocated, if resolved speculatively it can save at least 10 cycles for 1.4% of the branches ((100%-17.8%) x 1.7% = 1.4%, with 17.8% corresponding to the prediction rate of branches unresolved in cycle 16 and 1.7% the fraction of branches that remain unresolved after 16 cycles).

These savings are possible because as we see in Figure 3, almost all branches that are unresolved in cycle 16 remain unresolved until cycle 25. This benefit comes at the expense of increasing the delay for 0.3% of the branches ($17.8\% \times 1.7\% = 0.3\%$), who were initially predicted correctly but incorrectly resolved speculatively. Speculatively resolving branches early increases the opportunity for SBR as more branches are likely to remain unresolved but the accuracy of early resolution may be lower, hence rendering the overall approach detrimental. In the same vein, waiting to resolve speculatively later can help increase accuracy but at the expense of lower opportunity (as more branches are likely to be resolved already).

4. Speculative Branch Resolution

One key issue with using timing information is that it is usually not available at prediction time for many branches. As a result, our proposed technique, *Speculative Branch Resolution* or *SBR*, is an overriding scheme that re-predicts branches in the backend to be able to leverage more rich timing information.

4.1. Timing Information Vector

SBR re-predicts a branch instance using timing information of other branch instances. At a given time, the *timing* of a branch instance corresponds to the number of cycles it spent in the ROB unresolved (so far). Depending at which stage and when SBR re-predicts a branch, the timing information that is available for other branches varies.

First, at fetch, we can obtain the timing information of retired branches as well as older branches that are already in the ROB, that is, a subset of older branches. In this case, the timing information of branches older than the fetched branch that have not been added to the ROB is not available. Another point is just before a branch allocates an entry in the ROB, which we term *pre-alloc*. At this point, we can obtain the timing information of all the older branches in the ROB, as well as of retired branches. However, there is no timing information for branches that are younger as those branches have not yet reached the ROB. A last option is a few cycles after entering the ROB, which we term *post-alloc*. In this case, we have timing information about i) Retired branches ii) Older branches still in the ROB and iii) Younger branches that entered the ROB. Assuming the re-predicted branch was initially mispredicted, waiting longer to re-predict reduces the number of cycles saved, but enriches the available timing information. In this work, SBR re-predicts post-alloc, as this provides the richest set of information to the overriding predictor. We define the number of cycles we wait before re-predicting a branch after it entered the ROB as the *re-predict cycle*.

The *Timing Information Vector*, or *TIV*, used by the SBR predictor encodes the timing behavior of branches. A single bit of this information vector encodes whether a branch instance resolved fast or slow based on a *timing threshold*. This does not distinguish between a branch being resolved or unresolved, although a resolved branch will never change

category as time passes, while an unresolved branch may switch from fast to slow as cycles advance. The *TIV* is built from the concatenation of three sub-vectors:

Commit Timing Information Vector or CTIV is a vector that contains timing information regarding branches that have retired, hence have resolved. Each entry in CTIV denotes whether a branch resolved fast or slow.

Older Timing Information Vector or OTIV is a vector that contains timing information about branches that reside in the Reorder Buffer (ROB) and are older relative to the branch being re-predicted. Those can either be resolved or unresolved.

Younger Timing Information Vector or YTIV is a vector that contains timing information of branches that are in the ROB and are younger relative to the branch being re-predicted. Those can either be resolved or unresolved.

Our approach uses branch resolution timing as a proxy for various potential sources of delays (e.g., TLB/cache misses) because such events are reflected in resolution delays. This captures the combined impact of all the delay inducing events without explicitly modeling each individually, enabling us to evaluate the potential upper bounds of leveraging aggregate timing information for re-prediction. Future work can investigate the benefits of isolating the source of delays in the *TIV*.

Figure 4 shows an example of how a vector is constructed out of the ROB and the retired branch instructions, assuming re-predict cycle 4, CTIV and OTIV timing threshold of 8 and YTIV threshold of 2. The total size of the *TIV* for this example is assumed to be 9. The branch being re-predicted is highlighted in black. The younger branches are in green, the older but not yet committed are in blue, and the recently retired ones are in orange. We first check the number of cycles elapsed since allocation of younger branches, and determine whether they are fast or slow based on the *YTIV* threshold. For instance, although it is not resolved yet, the youngest (rightmost) one is considered fast because it has spent fewer cycles in the ROB unresolved than the *YTIV* threshold. Continuing, we go through all the branches in the ROB, except the re-predicted branch, and we set the bits in the *TIV*. If there are not enough branches in the ROB to complete the *TIV*, we go through the retired branches. For this example, we use 4 retired branches to fill the remaining slots in the *TIV*.

A subtlety of the *TIV* construction algorithm is that assuming it has length of n , we can always build it using information from the n most recent older branches by combining the OTIV and the CTIV. However, depending on timing, there may be an arbitrary number of younger instructions in the ROB. In practice, having more younger branches pushes out some bits from CTIV (and potentially OTIV), and makes two different *TIV* not directly comparable as the bit position that delineates older information from younger information, relative to the branch being re-predicted, varies. In addition, if the *YTIV* uses a different threshold, a branch may be considered slow in the *YTIV*, but fast when it moves to the *CTIV* or *OTIV*. Since the *TIV* is always of length n , this *TIV* construction algorithm

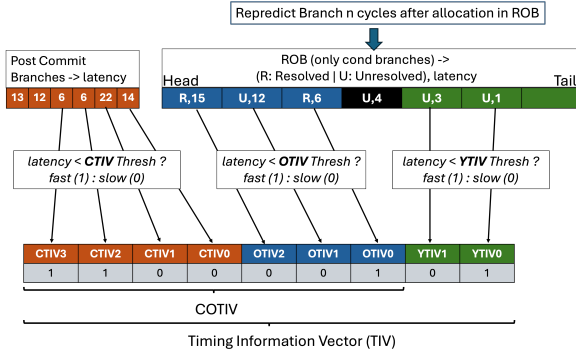


Figure 4: Example of how the Timing Information Vector is constructed (Re-predict cycle: 4, CTIV Threshold: 8, OTIV Threshold: 8, YTIV Threshold: 2)

"inconsistency" can help to encode how many elements of the TIV are from the YTIV vs. the CTIV/OTIV. We also observe that inserting the direction provided by the fetch predictor for the branch being re-predicted into the TIV is important to achieve better accuracy. Overall, the TIV vector combines the information in the following order: the commit vector, then the older vector, then the younger and finally the fetch prediction.

4.2. SBR Mechanism

Speculative Branch Resolution (SBR) re-predicts H2P branches post-allocation but before resolution, functioning as an overriding predictor [12, 14, 24]. The fetch predictor and the SBR overriding predictor we use are TAGE based and as a result, we differentiate between them as *Fetch TAGE* predictor, and the *SBR TAGE* predictor.

TAGE Predictor Primer. This predictor is depicted in Figure 5, borrowed from Seznec and Michaud [25]. To predict a branch direction, the PC of the branch is combined with the global branch history to form indices to the different tables, with the index to each tagged using different lengths of the global branch history, with the length growing geometrically. The prediction is provided by the component that uses the longest history and hits (the *provider* component). If there are no hits in the tagged component, the bimodal table provides the prediction. On a misprediction, an entry is allocated in a table that uses a longer history than the *provider*, either the immediate next table, or a random table. It is also possible to allocate multiple entries every time [21]. TAGE also uses the notion of *alternate* component, which is the table that hits and uses the second most longest history, i.e., it would have been the *provider* if the *provider* had missed.

SBR Overview. At the *re-predict* cycle, n , SBR TAGE is accessed using an information vector composed of the CTIV (recently committed branches), OTIV (older branches in the ROB) and YTIV (younger branches in the ROB) hashed with the branch PC. If i) SBR TAGE hits, ii) The prediction is different from the prediction of *Fetch TAGE*, and iii) The

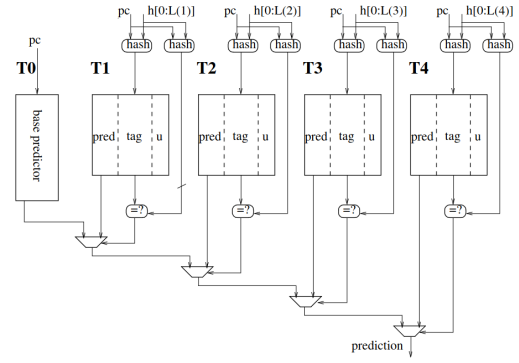


Figure 5: 5-component TAGE predictor synopsis: a base predictor is backed with several tagged predictor components indexed with increasing history lengths. From Seznec and Michaud [25].

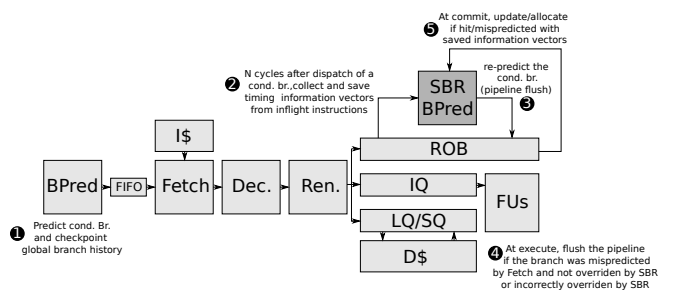


Figure 6: SBR (darker) and baseline (lighter) pipeline.

SBR prediction is confident, SBR overrides the *Fetch TAGE* prediction. If *SBR TAGE* misses then the branch is not re-predicted, but an entry is allocated in *SBR TAGE* if *Fetch TAGE* turns out to be incorrect. For update, we use the same policies as a normal TAGE predictor. Allocation takes place only when i) *Fetch TAGE* mispredicted and ii) *Fetch TAGE* accuracy on the entry SBR had a hit on has accuracy lower than a threshold, or when i) *Fetch TAGE* mispredicted and ii) *SBR TAGE* missed. The high level overview of a pipeline featuring SBR is depicted in Figure 6.

Furthermore, Figure 7 details the different cases in which SBR either does override fetch (orange arrows) or not (dark arrows). Note that SBR makes use of a heuristic to determine

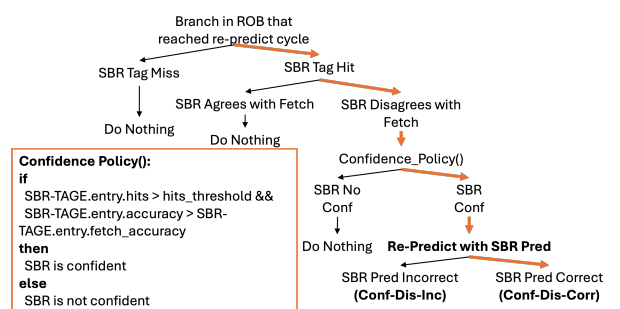


Figure 7: SBR TAGE override decision tree.

TABLE 1: PREDICTIONS CATEGORIES. OVERRIDE CASES ARE IN **BOLD ORANGE.**

SBR TAGE Hit					
Confident		NotConfident			
Agree with Fetch	Correct	Agree with Fetch	Correct		
	Incorrect		Incorrect		
Disagree with Fetch	Correct	Disagree with Fetch	Correct		
	Incorrect		Incorrect		

if the prediction of *SBR TAGE* should be preferred over *Fetch TAGE*. The confidence heuristic is listed in Figure 7 and considers counters about the accuracy of *Fetch TAGE* and *SBR TAGE*. Practically, *SBR TAGE* overrides *Fetch TAGE* in a single case, which is when *SBR TAGE* hits, disagrees with *Fetch TAGE*, and is confident according to the heuristic. In all other cases, *SBR TAGE* does not override, that is i) When it misses, ii) When it agrees with *Fetch TAGE*, or iii) When it is not confident according to the heuristic. Table 1 summarizes the different possibilities noting for each case that SBR can be correct or incorrect. Once SBR determines that it must override a branch, the pipeline is flushed and the frontend is resteeered to the other path of the conditional branch.

This is a double edged sword: If the branch was originally mispredicted by fetch and SBR correctly re-predicted it, then the branch resolution latency has been improved by X cycles, where X is the remaining cycles this branch would need to resolve without SBR. On the contrary, if the branch was originally correctly predicted by fetch and we re-predict it, latency increases by Y cycles, where Y is the pipeline refill penalty after a branch misprediction. As a result, although SBR has potential for saving many cycles it should be used judiciously.

5. Experimental Setup

TABLE 2: DESCRIPTION OF BENCHMARKS AND H2P BRANCHES

Benchmark	Total BMPKI	SC BMPKI	# of H2P	BMPKI H2P	Coverage
Blender	1.71	0.24	8	1.25	73%
Deepsjeng	3.37	0.53	10	1.43	42%
Exchange2	0.74	0.12	3	0.23	30%
Gcc	3.83	0.59	16	0.37	10%
Leela	8.68	1.14	17	5.54	64%
Mcf	19.93	3.34	9	17.84	90%
Omnetpp	3.22	0.61	3	2.51	78%
Wrf	1.09	0.13	5	0.36	33%
X264	1.23	0.20	5	0.74	60%
Xz	5.34	0.77	16	4.02	75%

5.1. SPEC2017 rate Benchmarks Characteristics

We evaluate SBR using SPEC2017 rate benchmarks [3] (compiled for x86_64 with gcc8 -O2). We selected 92 H2P branches from 10 high BMPKI (> 0.70 BMPKI) benchmarks. A H2P branch has more than 0.045 BMPKI and all selected H2P branches of one benchmark should have at least a cumulative misprediction coverage of 30%. One exception is *gcc*, as this benchmark has many unique instructions that have a high misprediction rate but are executed only a few times. Table 2 describes, for each benchmark, the global

BMPKI of *Fetch TAGE*, the BMPKI from the SC component of *Fetch TAGE*, the number of H2P branches we selected for each benchmark and the coverage of these H2P branches. We focus on re-predicting *Fetch TAGE* predictions that were provided by the TAGE components (including bimodal), as they represent the majority of the mispredictions.

5.2. Simulation Framework

We find representative regions of workloads following the Simpoint sampling methodology [9, 17]. We then replay these simpoints in *gem5* [15], using full-system mode (50M warm-up, 100M actual run). We model a detailed out-of-order pipeline resembling Intel Skylake (6-wide, 224 ROB, 97 IQ, 72 LQ, 56 SQ). The model features a decoupled frontend that implements Fetch Directed Instruction Prefetching (FDIP) with a 192-entry fetch target queue [19] and a very large (32M-entry tables) *Fetch TAGE-SC* branch predictor. The latter is used to minimize aliasing effects such that if SBR is able to capture behavior that TAGE-SC cannot, it will be because of a fundamental difference in the information it uses to predict, rather than because *Fetch TAGE-SC* suffers from aliasing. For cache prefetching we use the *tagged prefetcher* as we found it to be the best performing data prefetcher among all those currently available in *gem5*. The *SBR TAGE* predictor also uses very large tables and the same history length as the *Fetch TAGE*. However, *SBR TAGE* has neither bimodal table nor a SC component. Another difference is that *SBR TAGE* tables are updated/allocated only from the selected H2P branch but the history, as the original TAGE, is updated by all the branches.

5.3. Design Space Exploration

We explored all the combinations of the following parameters. We investigate the **re-predict cycle** used for SBR, to determine the number of branches eligible for SBR as well as the quality of the timing information available at specific re-predict cycles. We vary the **timing thresholds** of the different TIVs that determine whether resolution was fast or slow. We sweep a range from 2 to 128 cycles, in powers of 2. Note that the timing threshold for CTIV and OTIV is the same, but the YTIV threshold is different as its behavior is tied to the re-predict cycle. For example, if the re-predict cycle is 16, there is no reason to have a threshold above 16 for YTIV as all of YTIV bits will encode *fast*. As a result, when YTIV is included we explore the timing thresholds from 2 until the re-predict cycle in powers of 2.

We consider vector combinations using only older information (CTIV+OTIV) and using both older and younger information (CTIV+OTIV+YTIV). We also consider XOR-ing the overall TIV with the global branch history, as global history is known to be good at finding correlations between branches [6, 13, 16, 20, 22, 25, 28, 31].

We varied the allocation policy for *SBR TAGE*. Our scheme allocates in *SBR TAGE* on *Fetch TAGE* misprediction, but checks if the *Fetch TAGE* accuracy of an entry is below a threshold. The intuition behind this is that if a *Fetch TAGE* entry provides good accuracy, then there is no point for

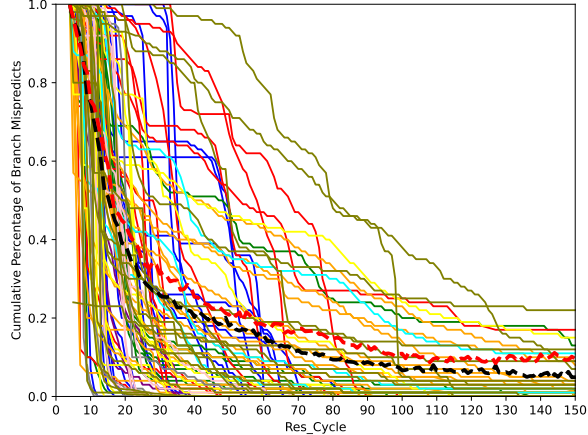


Figure 8: H2P mispredictions resolution cycle (coloured per benchmark) - Black dashed line is Skylake-Like core average - Red dashed line is Goldencove-Like core average

allocating an *SBR TAGE* entry for it. In our experiments, we considered 2 accuracy thresholds. First, the *Fetch TAGE* entry must have below 99% accuracy, as to never limit the allocations of SBR and train it quickly. Second, the *Fetch TAGE* entry must have below 80% accuracy, to filter out cases where *Fetch TAGE* is doing well enough.

6. Results

6.1. Branch Resolution Latency

We first show a characterization of the resolution latency (after entering the ROB) of the selected H2P branches when they mispredict. This is an important analysis as the SBR re-predict cycle is a tradeoff between how many H2P branches can be repredicted and how "populated" the timing information vector will be. Moreover, this analysis denotes the cycles we can potentially save for each H2P branch. Figure 8 depicts the cumulated percentage of resolution latencies of all 92 branches (truncated to 150 cycles), with all branches belonging to a given benchmark using the same color. The Figure also shows the average resolution cycle for H2P mispredictions for the Skylake-like and Goldencove-like cores with the black and red dashed lines respectively.

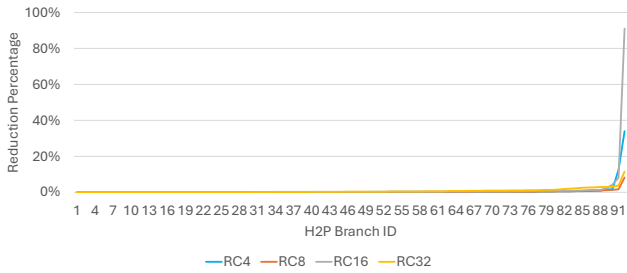


Figure 9: Misp. reduction when varying the re-predict cycle

Consider the uppermost line: Around 40% of the mispredictions for that branch are resolved within 70 cycles

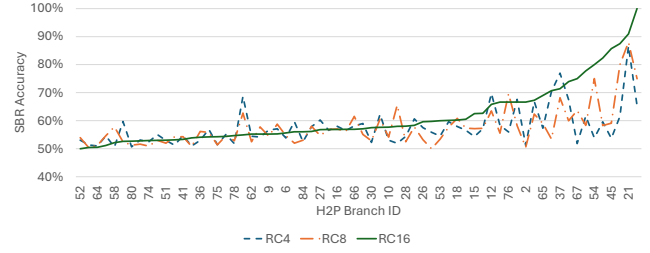


Figure 10: SBR accuracy with different re-predict cycles

after entering the ROB. This branch therefore has high potential for re-prediction, as we can repredict at cycle 70 and still have the opportunity to catch more than 60% of the mispredictions. On the other hand, focusing on the bottom left hand corner of the Figure, there are many branches for which 90% of the mispredictions are resolved within 10 cycles after entering the ROB. Those kind of branches do not provide much headroom for collecting timing information and re-predicting them. By considering the average, which is the dashed black line, it shows that 60% of the branch mispredicts are resolved within 20 cycles, while the red dashed line which is the Goldencove-like core shows that H2P branch mispredicts tend to take longer to resolve. In terms of saving cycles, based on the average we can save up to 20 cycles for the 40% of the branch mispredicts and up to 40 cycles for 20% of the branch mispredicts. Nevertheless, the figure also illustrates that each H2P branch has different behavior in term of resolution cycle, even within the same benchmark. Consider the blue lines, which belong to *leela*, we can observe both behaviors (fast and slow to resolve). This suggests that ideally, each PC would have to be re-predicted at a different time, even within a benchmark.

6.2. Analysis of SBR Potential

In this work, we aim to gauge the potential of SBR and therefore focus on performance analysis of an idealistic SBR mechanism on top of a baseline out-of-order pipeline, using cycle-level simulation.

6.2.1. Impact of re-predict Cycle. Figure 9 shows the misprediction reduction percentage for each re-predict cycle, for all the H2P branches, using the best configuration in the design space for each branch. The four lines of this figure are sorted separately, hence, the x-axis labels do not represent each a unique H2P branch: the same point across the lines can be a different H2P branch. The criterion for picking the best configuration is the largest misprediction reduction. We note that the H2P branch discussed in Section 3 sees a reduction of 91% at re-predict cycle 16 (*Fetch TAGE* misprediction rate is 82%). We also observe two cases where the reduction is 33% and 12% at re-predict cycle 4. The former is again for the same H2P branch. Nevertheless, the vast majority of the H2P branches do not benefit from SBR.

Figure 10 shows the *SBR TAGE* accuracy (y-axis) as a function of the re-predict cycle. Re-predict cycle 32 is not

shown as many H2P branches have resolved by that time, resulting in low potential overall. In general, we observe that waiting longer is beneficial, as the SBR accuracy tends to be highest with re-predict cycle 16. From Figure 10 onward, all figures with x-axis labeled as *H2P branch ID* are consistent, e.g., *H2P Branch ID* 21 denotes the H2P branch discussed in Section 3.

6.2.2. Performance of Best per-PC SBR Configurations.

Figure 11 reports the contribution of different classes of mispredictions for each of the 92 PCs, using the best timing vector configuration per PC. The 8 categories are the ones described in Table 1. We also show two lines which represent the *Fetch TAGE* accuracy (red line) and the *SBR TAGE* accuracy (black line).

The largest category corresponds to the case where *Fetch TAGE* was incorrect, *SBR TAGE* agrees with *Fetch TAGE* and *SBR TAGE* is not confident (NotConf-Agree-Inc). This suggests that either the mechanism or the predictor we use is not suitable for this kind of information, or the information we use fails to differentiate the mispredictions from the correct predictions. Another frequent case is BR-NotRepred, in which branch instances do not reach the re-predict cycle, confirming that many H2P branches often resolve fast (Figure 8). SBR is beneficial only in the *Conf Disa-Corr* category, which is limited and only covers more than 10% of the *Fetch TAGE* mispredictions for 3 branches.

It is interesting to note that 2 "winner" branches share the same best configuration, which uses COTIV only, meaning older branches, at re-predict cycle 4 and timing threshold 128 cycles. This is not unexpected as those two branches are in the same function, *spec_qsort* (one is branch A, number 21), suggesting that both H2P branches share the same timing behavior, and that SBR is able to capture it. We also analysed some of the non-beneficial H2P branches best configurations and most of them use the configuration that XORs the global branch history with the TIV. This suggests that for those branches, timing does not correlate with branch directions, and adding the ghst simply allows *SBR TAGE* to reach the same conclusions as *Fetch TAGE*.

6.2.3. Why SBR is not working.

We explain the limitations of timing information using a H2P branch from omnetpp for which SBR offers no advantage. Listing 2 shows the code of the function *shiftup* and of the inline operator "`<=`". The *shiftup* restructures the heap, denoted by table *h[]* in the listing, and uses the inline operator for deciding the order relation between heap elements. The elements are *cMessages* which can represent events, messages, jobs or other entities in a network simulation. We analyzed the branch in Line 22. This branch is part of a series of checks that first compare the timestamps (Lines 19,20) to determine if the messages occurred at different times. If the timestamps are identical, the branch compares the scheduling priorities of the messages (Lines 21,22), which are derived from the input *cMessages*. These priorities are a function of the *cMessages* and the specific heap configuration. This means that the branch outcome is

determined by the data characteristics of messages, i.e., is data dependent. First, Figure 12 establishes the lack of self timing correlation of the branch in Line 22, by showing that its *Fetch TAGE* accuracy is insensitive to its resolution cycle.

```

1 void cMessageHeap::shiftup(int from){
2     // restores heap structure (in a sub-heap)
3     int i = from, j;
4     cMessage *temp;
5     while ((j < i) <= n){
6         if ((j < n & (*h[j] > *h[j+1])) //direction
7             j++;
8         if (*h[i] > *h[j]){ //is change necessary?
9             temp=h[j];
10            (h[j]=h[i])->heapindex=j;
11            (h[i]=temp)->heapindex=i;
12            i=j;
13        }
14        else
15            break;
16    }
17 }
18 inline int operator <= (cMessage& a, cMessage& b){
19     return (a.getArrivalTime() < b.getArrivalTime()) ? 1 :
20     (a.getArrivalTime() > b.getArrivalTime()) ? 0 :
21     (a.getSchedulingPriority() < b.getSchedulingPriority()) ? 1 :
22     (a.getSchedulingPriority() > b.getSchedulingPriority()) ? 0 :
23     a.getInsertOrder() <= b.getInsertOrder();
24 }
```

Listing 2: Source code of *shiftup* in *omnetpp*

Second, to investigate why timing correlation with other branches is not useful for this branch, we analyzed the correlation of the direction of this branch with its TIV vectors. We used TIV vectors that include the ten most recent branches from COTIV and YTIV at repredict cycle 8 (we checked various vector lengths, but the conclusions remained the same). Older branches include those at Lines 19–21 (always executed before Line 22), while younger branches include Line 23 and branches from subsequent iterations. For each unique vector we count how often the branch is taken and not-taken to determine a vector's SBR bias, defined as the most popular direction divided by the total vector frequency.

The scatter plot in Figure 13 compares the SBR bias against the *Fetch TAGE* accuracy for each vector. Points along the diagonal (black line) indicate that SBR TIVs do not glean any additional correlation. We observe that for the *omnetpp* branch, all vectors align with the diagonal, confirming the lack of additional correlation from the use of timing information as compared to *Fetch TAGE*.

For the *H2P Branch ID* 58 (Branch at Line 22), Figure 11 shows that the portion of mispredicts where SBR agrees with the fetch predictor (green segment) dominates, along with the portion where SBR disagrees but it's not confident enough to re-predict (orange segment). This confirms that timing information does not help capture better the correlation behavior of this branch as compared to *Fetch TAGE*.

We also perform the bias analysis, for the H2P branch in *mcf* (Section 3), using only older branches at repredict cycle 4. Younger branches do not improve the SBR accuracy for this branch for any SBR configuration we evaluated. In contrast to the branch from *omnetpp*, Figure 13 reveals that *mcf* has vectors well above the diagonal, indicating cases where SBR can improve over *Fetch TAGE* by leveraging timing information.

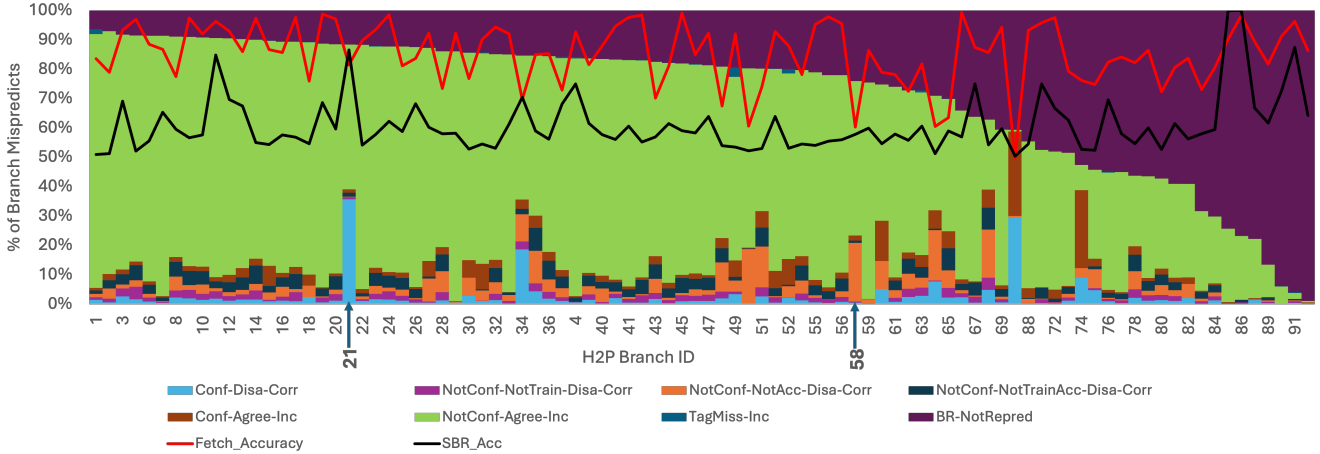


Figure 11: Results of gem5 simulations (Point 21 is mcf branch A introduced in Section 3)

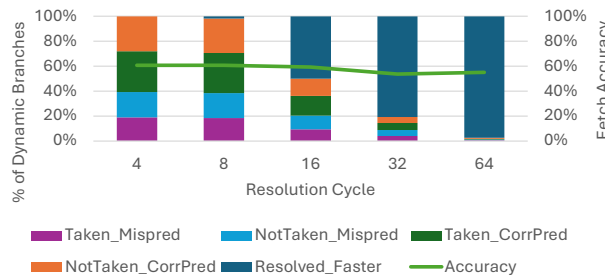


Figure 12: Taken and Not-Taken Correct Predictions and Mispredictions for an omnetpp branch as a function of resolution time

6.2.4. Goldencove Analysis. The temporal behavior of instructions in the pipeline depends on the microarchitecture. Hence, we study the impact of larger structures on SBR using a Goldencove-Like core. This core is 8-wide with 512 ROB entries, 220 IQ entries, 172 LQ and 156 SQ entries, 350 integer and 330 floating-point registers.

We explored the same design space in terms of *SBR TAGE* configurations, and we observed (results not shown due to space limitations) that with a larger window, SBR accuracy tends to be slightly higher, although SBR remains unable to provide gains except in few specific cases. However, H2P branches tend to take slightly longer to resolve with a longer instruction window, as seen in Figure 8, suggesting more SBR opportunity with a larger window in terms of how many instances can be re-predicted before a given re-predict cycle.

7. Conclusion

This paper set out to explore if using new information that is available later in the pipeline – timing information – can help re-predict hard-to-predict (H2P) branches with better accuracy. The main conclusion is that the information we considered, as leveraged by a TAGE predictor, cannot

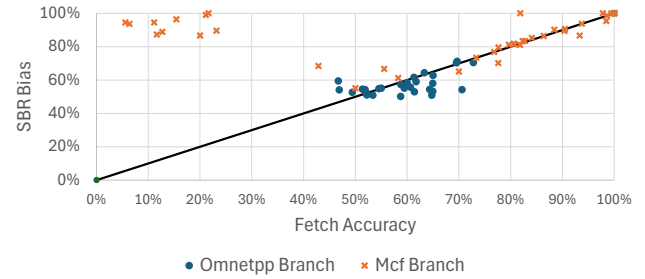


Figure 13: Scatter plot of vectors encoded with 1 and 0 based on resolution cycles for omnetpp H2P branch and mcf H2P branch - The black line is a reference of the diagonal

beat a large TAGE-SC predictor that only uses architectural information except in very specific cases.

Although the result is generally negative, i.e., timing as defined in this work rarely correlates with higher accuracy to branch outcome as compared to a large TAGE-SC, we identified two H2P branches that benefit from timing information, and provided an in-depth analysis as to why the timing information is useful for one of them. As a result, this study can serve as a starting point for SBR-like mechanisms that use a different kind of post-fetch microarchitectural information. We have also observed that while some H2P branches usually take a long time to resolve, the average resolution time (allocation in ROB to execution) is below 20 cycles for 50% of the H2P branches studied in this work. As a result, future work may consider using microarchitectural information available earlier in the pipeline to refine existing overriding predictors [12].

References

[1] M. Al-Otoom, E. Forbes, and E. Rotenberg, “Exact: Explicit dynamic branch prediction with active updates,” in *Proc. of the Intl Conf. on Computing Frontiers*, 2010, pp. 165–176.

[2] D. N. Armstrong, H. Kim, O. Mutlu, and Y. N. Patt, "Wrong path events: Exploiting unusual and illegal program behavior for early misprediction detection and recovery," in *Proc. of the IEEE/ACM Intl. Symp. on Microarchitecture*. IEEE, 2004, pp. 119–128.

[3] J. Bucek, K.-D. Lange, and J. v. Kistowski, "Spec cpu2017: Next-generation compute benchmark," in *Companion of the ACM/SPEC Intl. Conf. on Performance Engineering*, 2018, pp. 41–42.

[4] A. Chauhan, J. Gaur, Z. Sperber, F. Sala, L. Rappoport, A. Yoaz, and S. Subramoney, "Auto-predication of critical branches," in *Proc. of the ACM/IEEE Intl. Symp. on Computer Architecture*. IEEE, 2020, pp. 92–104.

[5] A. N. Eden and T. Mudge, "The yags branch prediction scheme," in *Proc. of the IEEE/ACM Intl. Symp. on Computer Microarchitecture*. IEEE, 1998, pp. 69–77.

[6] A. Falcón, J. Stark, A. Ramirez, K. Lai, and M. Valero, "Prophet/critic hybrid branch prediction," in *Proc. of the ACM/IEEE Intl. Symp. on Computer Architecture*, vol. 1063, no. 6897/04, 2004, pp. 20–00.

[7] M. Goudarzi, R. Azimi, J. Humecki, F. Rehman, R. Zhang, C. Sethi, T. Bomman, and Y. Yang, "By-software branch prediction in loops," *IEEE Computer Architecture Letters*, vol. 22, no. 02, pp. 129–132, jul 2023.

[8] B. Grayson, J. Rupley, G. Z. Zuraski, E. Quinnell, D. A. Jiménez, T. Nakra, P. Kitchin, R. Hensley, E. Brekelbaum, V. Sinha *et al.*, "Evolution of the samsung exynos cpu microarchitecture," in *Proc. of the ACM/IEEE Intl. Symp. on Computer Architecture*. IEEE, 2020, pp. 40–51.

[9] G. Hamerly, E. Perelman, J. Lau, and B. Calder, "Simpoint 3.0: Faster and more flexible program phase analysis," *Journal of Instruction Level Parallelism*, vol. 7, no. 4, pp. 1–28, 2005.

[10] D. A. Jiménez, "Fast path-based neural branch prediction," in *Proc. of the IEEE/ACM Intl. Symp. on Microarchitecture*. IEEE, 2003, pp. 243–252.

[11] ——, "Multiperspective perceptron predictor," in *5th JILP Workshop on Computer Architecture Competitions (JWAC-5): Championship Branch Prediction (CBP-5)*, 2016.

[12] D. A. Jiménez, S. W. Keckler, and C. Lin, "The impact of delay on the design of branch predictors," in *Proc. of the IEEE/ACM Intl. Symp. on Microarchitecture*, 2000, pp. 67–76.

[13] D. A. Jiménez and C. Lin, "Dynamic branch prediction with perceptrons," in *Proc. of the IEEE Intl. Symp. on High-Performance Computer Architecture*. IEEE, 2001, pp. 197–206.

[14] G. H. Loh, "Revisiting the performance impact of branch predictor latencies," in *Proc. of the IEEE Intl. Symp. on Performance Analysis of Systems and Software*. IEEE, 2006, pp. 59–69.

[15] J. Lowe-Power, A. M. Ahmad, A. Akram, M. Alian, R. Amslinger, M. Andreozzi, A. Armejach, N. Asmussen, B. Beckmann, S. Bharadwaj *et al.*, "The gem5 simulator: Version 20.0+," *arXiv preprint arXiv:2007.03152*, 2020.

[16] S. McFarling, "Combining branch predictors," Citeseer, Tech. Rep., 1993.

[17] H. Patil, C. Pereira, M. Stallcup, G. Lueck, and J. Cownie, "Pinplay: a framework for deterministic replay and reproducible analysis of parallel programs," in *Proc. of the IEEE Intl Symp. on Code Generation and Optimization*, 2010, pp. 2–11.

[18] J. Pierce and T. Mudge, "Wrong-path instruction prefetching," in *Proceedings of the 29th Annual ACM/IEEE International Symposium on Microarchitecture*, 1996, p. 165–175.

[19] G. Reinman, B. Calder, and T. Austin, "Fetch directed instruction prefetching," in *Proc. of the IEEE/ACM Intl. Symp. on Microarchitecture*. IEEE, 1999, pp. 16–27.

[20] A. Seznec, "A 256 kbits L-TAGE branch predictor," *Journal of Instruction-Level Parallelism (JILP) Special Issue: The Second Championship Branch Prediction Competition (CBP-2)*, vol. 9, pp. 1–6, 2007.

[21] ——, "A 64 kbytes isl-tage branch predictor," in *JWAC-2: Championship Branch Prediction*, 2011.

[22] ——, "TAGE-SC-L branch predictors," in *JILP-Championship Branch Prediction*, 2014.

[23] ——, "Exploring branch predictability limits with the mtage+ sc predictor," in *5th JILP Workshop on Computer Architecture Competitions (JWAC-5): Championship Branch Prediction (CBP-5)*, 2016, p. 4.

[24] A. Seznec, S. Felix, V. Krishnan, and Y. Sazeides, "Design tradeoffs for the alpha ev8 conditional branch predictor," in *Proc. of the ACM/IEEE Intl. Symp. on Computer Architecture*. IEEE Computer Society, 2002, pp. 0295–0295.

[25] A. Seznec and P. Michaud, "A case for (partially) tagged geometric history length branch prediction," *The Journal of Instruction-Level Parallelism*, vol. 8, p. 23, 2006.

[26] A. Seznec, J. S. Miguel, and J. Albericio, "The inner most loop iteration counter: a new dimension in branch history," in *Proc. of the IEEE/ACM Intl. Symp. on Microarchitecture*, 2015, pp. 347–357.

[27] R. Sheikh, J. Tuck, and E. Rotenberg, "Control-flow decoupling," in *Proc. of the IEEE/ACM Intl. Symp. on Microarchitecture*. IEEE, 2012, pp. 329–340.

[28] J. Smith, "A study of branch prediction strategies," in *Proc. of the ACM/IEEE Intl. Symp. on Computer Architecture*, 1981.

[29] D. Tarjan and K. Skadron, "Merging path and gshare indexing in perceptron branch prediction," *ACM transactions on architecture and code optimization*, vol. 2, no. 3, pp. 280–300, 2005.

[30] T.-Y. Yeh and Y. N. Patt, "Two-level adaptive training branch prediction," in *Proc. of the IEEE/ACM Intl. Symp. on Microarchitecture*, 1991, pp. 51–61.

[31] S. Zangeneh, S. Pruitt, S. Lym, and Y. N. Patt, "Branchnet: A convolutional neural network to predict hard-to-predict branches," in *Proc. of the IEEE/ACM Intl. Symp. on Microarchitecture*. IEEE, 2020, pp. 118–130.

[32] C. B. Zilles and G. S. Sohi, "Understanding the backward slices of performance degrading instructions," in *Proceedings of the 27th Annual International Symposium on Computer Architecture*, 2000, p. 172–181.